A MULTI-BAND MEANDERED SLOTTED-GROUND-PLANE RESONATOR AND ITS APPLICATION OF LOW-PASS FILTER

C. J. Wang* and T. H. Lin

Department of Electrical Engineering, National University of Tainan, Tainan 700, Taiwan

Abstract—A slotted-ground-plane meandered-slot resonator with multi-resonance characteristics and a compact lowpass filter (LPF) by using the resonator are demonstrated in this paper. The meandered slot provides a wideband resonator with low insertion loss and very sharp cutoff frequency response. Unlike conventional design of cascading bandstop slotted-ground-plane resonators in the literature, the introduced LPF is presented, which consists of a modified-meander slot in the ground plane, a spurred C-like slot, and a uniform microstrip transmission line with constant characteristics impedance. Two rectangular-head slots, giving an increase in the inductance, are added at the two terminals of the meandered slot for purpose of frequency reduction. An arm aperture is embedded to form another resonant path so that an additional transmission zero could be generated. In order to increase rejection capability, the slot width of one section of the meandered-slot resonator is widened. Meanwhile, a C-like slot with a spur slit is also etched inside the meandered slot to improve rejection performance. The measured insertion loss at a passband is below 0.7 dB, and the rejection band over 20 dB is from 2.9 to 12.0 GHz.

1. INTRODUCTION

A patterned slot of a slotted-ground-plane resonator disturbs the surface current distribution in a ground plane and the impedance characteristics of a transmission line are changed [1]. At the resonant frequency, energy on the transmission line is stored in the slot and a band gap appears in the transmission characteristics. The signal at the specified frequency is blocked and the stopband performance is

achieved, and thus the bandstop resonator is designed. By employing circuit analysis theory, an equivalent resonance circuit of the slotted-ground-plane resonator is derived and lumped-element parameters are extracted. The lumped elements construct an LC tank, and then a stopband effect is obtained. When changing the shape of a slot, the equivalent inductance and capacitance could be tuned so that the frequency response of the transmission line is controlled.

Recently, slotted-ground-plane resonators in the low-pass filter have attracted much attention [1–20] because they have numerous advantages like circuitry size reduction and spurious response suppression. By cascading several equilateral resonator units, a low-pass filter with large size can be demonstrated. The units offer a finite-transmission-zero characteristics and the transmission zeros are used to suppress the spurious response of the low-pass filter. For most of the cases, a stepped-impedance (SI) topology or a gap is required to be utilized in the design of the transmission line above the slotted-ground-plane low-pass filter [1–5, 11]. In [3], a low-characteristic-impedance transmission line is placed on the top of the slotted ground plane. The SI transmission line has a capacitive element equivalently. Three dumbbell-shaped slots of different size are serially etched in the ground plane and provide three series inductor. A compact low-pass filter by using a quasi-π slot as a basic resonant circuit and four stepped-impedance shunt stubs are employed as harmonic-suppressed elements of the LPFs in [11]. Due to a resonator of high quality factor and narrow stop band, the meandered (interdigital) slot is usually used to introduce transmission zeros to the filter response and consequently improve its harmonic-rejection performance [18].

In the first part of this paper, a meander-shaped slotted-ground-plane resonator is shown to perform multi-band rejection characteristics in frequency response. Unlike a conventional slot in a ground plane acting a bandstop resonator, a modified-meander slot possesses multi-band frequency-rejection characteristics with a sharp transition knee. The phenomenon the rejection bands are theoretically analyzed by utilizing magnetic field distribution. Detailed discussions for important dimensional parameters are determined. In the second part, we propose a compact low-pass filter by using the meander-shaped slot as a basic resonant circuit. A transmission zero, which is resonated by a U-like slot path, is observed so that the proposed filter exhibits sharp cutoff frequency response. Similarly to add a perturbation stub in the resonator [19], an arm aperture is embedded in the meandered slot so that an additional transmission zero could be achieved. By changing geometries of the meandered slot and adjusting their impedance characteristics of the resonances properly without

affect the original low-pass characteristics of the slotted-ground-plane resonator, wideband harmonic suppression is obtained. Finally, a *C*-like slot with a spur slit, which provides two controllable transmission zeros, enhances the rejection performance.

2. A SLOTTED-GROUND-PLANE MEANDERED RESONATOR

2.1. Design and Results

As shown in Figure 1(a), for the wideband slotted-ground-plane resonator operated about at $3.0\,\text{GHz}$, an meandered-shaped slot etched in the ground plane and the dimensions of the slot are as following: $a = 20\,\text{mm}$, $d = 12\,\text{mm}$, $g = 1\,\text{mm}$, $t_1 = 5\,\text{mm}$ and $t_2 = 6\,\text{mm}$. The circuits in this paper are designed and fabricated on a high frequency printed circuit board FR4 with a relative dielectric constant of 4.4 and a thickness of $0.8\,\text{mm}$. The width of the transmission line is chosen for

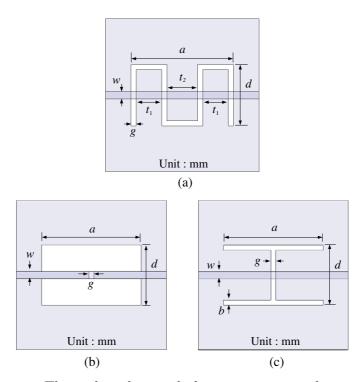(a)

(b)   (c)

Figure 1. Three slotted-ground-plane resonators, where $a = 20$, $d = 12$, $w = 1.5$, $g = 1$, $b = 1$, $t_1 = 5$, $t_2 = 6$. (a) Proposed meandered slotted-ground-plane resonator. (b) Dumbbell-shaped resonators. (c) H-shaped resonators.

the characteristic impedance of a 50-Ω microstrip line. In Figure 2, the simulated S-parameters of the meandered-shaped slot resonator are compared with the conventional dumbbell-shaped and H-shaped resonators (seeing Figures 1(b) and (c)) having same size. The first resonance frequencies of the H-shaped and meander-shaped resonators are operated about at 3.0 GHz. The first resonance frequency of the dumbbell-shaped resonator is resonated at 3.65 GHz. The 10-dB rejection bandwidth of the meander-shaped slot resonator is 3.14 GHz wider than those (2.48 and 1.21 GHz) of the dumbbell-shaped slot and H-shaped slot resonators. It is also observed that the attenuation rate and the harmonic suppression of the meandered-shaped resonator are superior to the other ones.
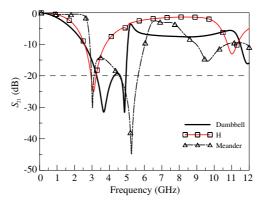

Figure 2. Simulated S_{21} of the meandered-shaped slot, dumbbell-shaped slot and H-shaped slot resonators.
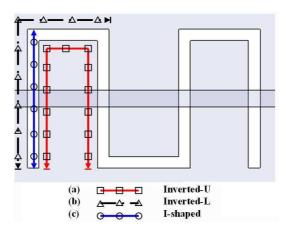

Figure 3. Three resonant paths of the meandered-slot resonator.

2.2. Resonance Analysis

In our experiment, we have undertaken such a numerical study with help of the 3-D EM simulator Ansoft HFSS v. 10, licensed by the National Center for High Performance Computing, Hsinchu, Taiwan. As shown in Figure 2, below 12 GHz, there are three resonances for the meander-shaped resonator. The three resonances are at 3.3, 5.3 and 9.6 GHz, which are excited by the inverted-U, inverted-L and I paths shown in Figure 3. Figure 4 is the simulated S_{21}-parameters of the slotted-ground-plane resonators for different slot topologies, including the meandered, inverted-U, inverted-L and I resonators. From the simulated results, the lower transmission zero at 3.0 GHz is excited by the inverted-U slot, the second transmission zero is generated by the inverted-L slot, and the third transmission zero is determined by the I slot. The discrepancy of the resonance frequency between the single and meandered resonators may be attributed to the mutual coupling effect of the slot trace. Figure 5 is the distributions of the magnetic filed of the meandered resonator at 3.3, 5.3 and 9.6 GHz. It is found that, for the magnetic field, a distance between two maximum out-of-phase vectors is half-wavelength, which is the resonant path of the slotted-ground-plane resonator. With reference to the figure, the distributions of the magnetic field theoretically explain the mechanism of the transmission zeros of the meandered-slot resonator.
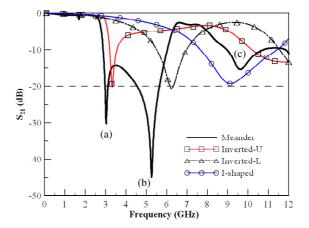

Figure 4. Simulated S_{21}-parameters of the slotted-ground-plane resonators, including the meandered, inverted-U, inverted-L and I resonators.
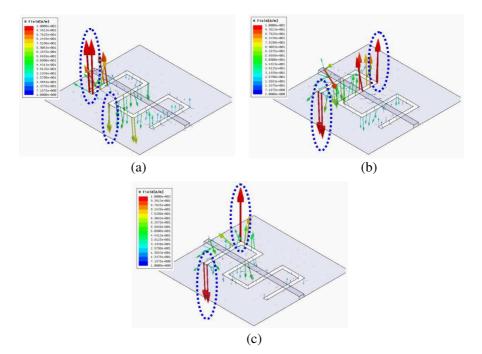
(a)

(b)

(c)

Figure 5. Distributions of the magnetic filed of the meandered resonator at three different operated frequencies. (a) 3.3 GHz. (b) 5.3 GHz. (c) 9.6 GHz.

2.3. Parametrical Study

The linewidth was chosen to be the characteristic impedance of 50-Ω microstrip line for simulation. In order to investigate the influence of the slot width which is related to the gap capacitance, the whole dimension of the meandered resonator was kept constant to $20 \times 12\,\text{mm}^2$ for all three cases.

It is noted that increasing the slot width (g) results in decrease of t_2 when t_1 is fixed. The simulated results are illustrated in Figure 6. From this figure, one clearly observes that decreasing the slot width increases the effective capacitance of the resonator which introduces the cutoff characteristics at transmission zeros. As the etched width of the slot is decreased, the effective capacitance increases, and it gives rise to a lower cutoff frequency, as seen in Figure 6. An additional transmission zero is excited around 1.8 GHz because of the resonance of the whole meandered slot path. The additional transmission zero is insignificant and useless so that it should be avoided to be excited.

We now investigate the influence of the resonant slot path, which is to change the lengist of t_1 with same dimension ($20 \times 12\,\text{mm}^2$) of the
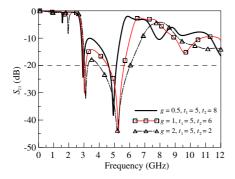
Figure 6. Comparison of simulated transfer characteristics of the meandered resonator when changing the slot width (g).
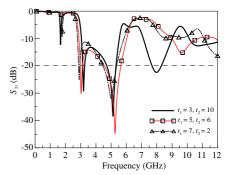
Figure 7. Simulated transfer characteristics of the test circuit by varying t_1 when the slot width (g) is fixed by 1 mm.

whole unit circuit. Note that g is fixed by 1 mm and t_2 is varied. The simulated transfer characteristics of the test circuit by varying t_1 are shown in Figure 7. The additional transmission zero around 1.8 GHz is easily generated for two cases of $t_1 = 3$ and 5 mm. Due to the increase of the resonant path of the inverted-U resonator, the transmission zero at 3.0 GHz shifts down as t_1 increases. It is interesting that the resonance frequency of the transmission zero at 5.3 GHz also reduces when t_1 is 3 mm. The reason of this phenomenon results from the change of the resonator at this operated frequency. The resonant path for large t_1 is inverted-L, but one for small t_1 is inverted-J. When t_1 changes from 5 mm to 3 mm, one maximum magnetic fields is moved from the right corner of the inverted-U slot to the cross point of the microstrip line and the slot. The resonant path increases so that the frequency reduction of the transmission zero is achieved.

3. DESIGN OF THE LOW-PASS FILTER

3.1. Design

Compared to the other topologies, the meandered resonator possesses a wide rejection bandwidth in frequency characteristics. In our design in Figure 1(a), several techniques to excite additional transmission zeros and to enhance bandstop performance to demonstrate a low-pass filter are as shown in Figure 8(a). As we know that a patterned slot in the ground plane disturbs the surface current distribution of the ground plane and thus the impedance characteristics of a transmission line are changed, a transmission zero (or called an attenuation pole)

could be excited. First, an aperture with the length of p_l is embedded inside the inverted-U slot at the left of the meandered-slot resonator. According to the mechanism of the slotted-ground-plane resonator, another inverted-L resonant path can cause an additional transmission zero. The slot-head area basically controls the inductance. By changing the etched area of the aperture, the internal reactance of the resonator is modified so that the frequency characteristics could be improved.

As similar as the previous technique, the slot width of one section of the meandered-slot resonator is widened. In order to compensate the frequency movement resulting from the above techniques, two rectangular-head slots, giving an increase in the inductance, are added at the two terminals of the meandered slot for purpose of frequency reduction. Finally, a C-like resonator with a spur slit is embedded inside the modified meandered resonator to achieve a good harmonic-rejection performance of $S_{21} < -20\,\text{dB}$. The modified C-like resonator provides dual-band rejection characteristics. The fundamental rejection band of the embedded resonator is controlled by the C-like trace path and; on the other hand, the harmonic band is varied by the spur slit. The schematic diagram and the dimensional parameters of the spurred C-like slot are shown in Figure 8(b).
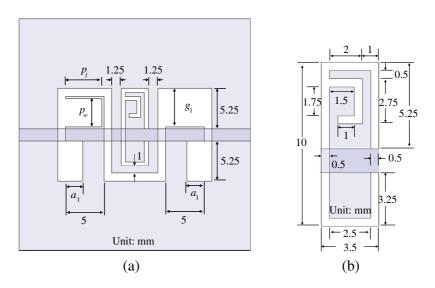

Figure 8. Schematic diagrams of the proposed low-pass filter and the embedded spurred C-like resonator. (a) Low-pass filter. (b) Spurred C-like slot resonator.

3.2. Results

Figure 9 shows the effects of the length (p_l) of the embedded aperture on the scattering parameter S_{21} for the meandered slot, respectively. The width (p_w) of the additional slot is fixed by 1 mm. The area and other dimensions of the meandered slot are kept equal. The extra aperture connected at the inverted-U resonator provides a new transmission zero, which is controlled by the small additional inverted-L slot, around 8.0 GHz. The location of the transmission zero and the higher rejection band shifts down with an increase of p_l. The harmonic suppression of the stopband is better for the meandered resonator. There is a small effect in the lower rejection bandwidth a change of p_l. Figure 10 shows dependence of the resonance frequency on the width (p_w) of the aperture with $p_l = 4.75$ mm. We see in the figure that for large width (p_w) of the slot head, the small inverted-L slot provides better sharpness of cutoff with improved stopband response at the additional transmission zero around 8.0 GHz. The lower rejection band is slightly affected. Figure 11 plots the simulated impedance locus of two meandered slots with $p_w = 1$ mm and $p_w = 3.75$ mm on the Smith chart at 9.43-GHz band. The increase of p_w results in a moving-out variation of the input impedance and an improvement of harmonic suppression.

Figure 12 shows the comparison of the frequency characteristics of the resonator, where the width (g_1) of the one section of the meandered slot changes from 1 mm to 5.25 mm. In the parametrical study of Section 2, it is found that the rejection capability of the resonator enhances when increasing the width of the slot gap. From the results, the frequency-rejection response from 6.0 GHz to 11 GHz is improved
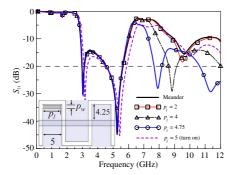

Figure 9. Effects of the length (p_l) of the embedded aperture on the scattering parameter S_{21} for the meandered slot.
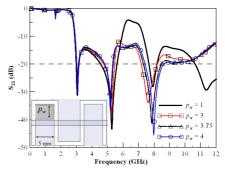
Figure 10. Dependence of the resonance frequency on the width (p_w) of the aperture with $p_l = 4.75$ mm.
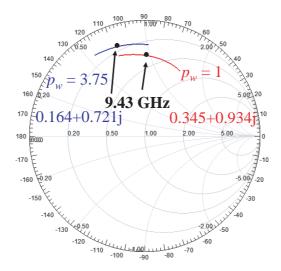
Figure 11. Simulated impedance locus of two meandered slots with $p_w = 1$ mm and $p_w = 3.75$ mm on the Smith chart at 9.43-GHz band.
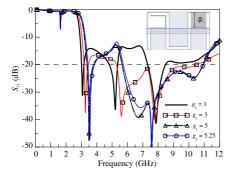

Figure 12. Comparison of the frequency characteristics of the resonator, where the width (g_1) of the one section of the meandered slot changes from 1 mm to 5.25 mm.
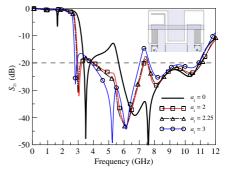

Figure 13. Simulated frequency response of the modified meandered slot with two rectangular-head slots whose dimension is $a \times 5.25$ mm^2.

as predicted. However, the spurious frequency at 1.8 GHz becomes large with an increase of g_1. The first resonant band shifts slightly up. In order to modify the frequency change, two rectangular-head slots are etched at the two terminals of the meandered slot. Figure 13 shows the simulated frequency response of the modified meandered slot with two rectangular-head slots whose dimension is $a \times 5.25$ mm^2. For the case of $a = 2.5$ mm, the initial cutoff frequency does not move up
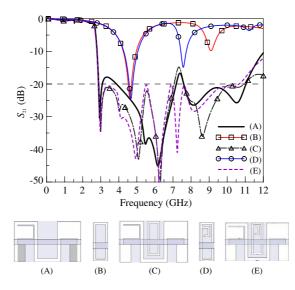
Figure 14. Simulated S_{21} of the five resonators, including the modified meandered slot (A), the C-like slot (B), the meandered slot with the C-like slot (C), the C-like slot with the spur slit (D), and the meandered slot with the spurred C-like slot (E).

from 3.4 GHz to 2.9 GHz, but the spurious frequency also decreases. In order to achieve a rejection level of -20 dB, there are still two frequency bands about 3.1 GHz and 7.5 GHz to be suppressed.

Figure 14 shows the simulated S_{21} of the different resonators, including the modified meandered slot, the C-like slot, the meandered slot with the C-like slot, the C-like slot with the spur slit, and the meandered slot with the spurred C-like slot. As seen in the figure, the addition of the spur slit changes the harmonic resonant band without affecting the fundamental resonant band determined by the C-like slot. After embedding the spurred C-like slot in the modified meandered slot, the two peak frequency points at 3.1 GHz and 7.5 GHz have been suppressed below -20 dB. The frequency response of the resonator achieves a low-pass filter. The comparison of simulated and measured S-parameters of the simple meandered-slot resonator and the proposed low-pass filter is shown in Figure 15. As shown, reasonable agreement among the results is obtained. The designed slotted-ground-plane LPF exhibits a much shaper transition knee than the conventional ones which are fabricated by using a cascade form. Its transition bandwidth from 1 to 20 dB attenuation is only 0.37 GHz. The measured passband insertion loss is almost less than 0.7 dB. The stop bandwidth corresponding to 20 dB rejection is from 2.9 GHz to
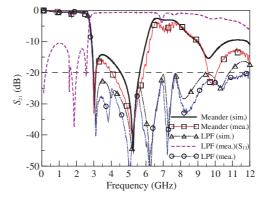
Figure 15. Comparison of simulated and measured S-parameters of the simple meandered-slot resonator and the proposed low-pass filter.

12.0 GHz. The total length of the proposed LPF is 20 mm, and compared with the LPF reported in [20], it is reduced about 24.8%.

4. CONCLUSION

In this paper, a wide stopband meandered slotted-ground-plane resonator and a compact low-pass filter with a uniform transmission line have been demonstrated. Compared to the other patterned slot, the meandered-slot resonator has wide rejection bandwidth and high attenuation rate. For the low-pass filter, sharp cutoff frequency response and low-pass characteristics are achieved by a modified meandered slot and an embedded spurred C-like slot. By utilizing two practical techniques, including connecting a rectangular aperture to the meandered slot and changing the slot width of one section of the slot, the capability of harmonic suppression improves. The C-like slot is embedded inside the meandered slot to enhance the rejection characteristics to achieve an attenuation level of 20 dB. Two rectangular-head slots are added at the two terminals of the meandered slot such that the initial cutoff frequency of the LPF could be reduced. The property of the uniform transmission line for the proposed structure can find more applications in the wireless communication systems.

ACKNOWLEDGMENT

REFERENCES

1. Park, J. S., J. S. Yun, and D. Ahn, "A design of the novel coupled-line bandpass filter using defected ground structure with wide stopband performance," *IEEE Trans. Microw. Theory Tech.*, Vol. 50, No. 9, 2037–2043, Sep. 2002.

2. Lim, J. S., C. S. Kim, Y. T. Lee, D. Ahn, and S. Nam, "Design of lowpass filters using defected ground structure and compensated microstrip line," *Electron. Lett.*, Vol. 38, No. 22, 1357–1358, Oct. 2002.

3. Abdel-Rahman, A. B., A. K. Verma, A. Boutejdar, and A. S. Omar, "Control of bandstop response of Hi-Lo microstrip low-pass filter using slot in the ground plane," *IEEE Trans. Microw. Theory Tech.*, Vol. 52, No. 3, 1008–1013, Mar. 2004.

4. Ting, S. T., K. W. Tam, and R. P. Martins, "Miniaturized microstrip lowpass filter with wide stopband using double equilateral U-shaped defected ground structure," *IEEE Microw. Wireless Comp. Lett.*, Vol. 16, No. 5, 240–242, May 2006.

5. Chen, H. J., T. H. Huang, C. S. Chang, L. S. Chen, N. F. Wang, Y. H. Wang, and M. P. Houng, "A novel cross-shaped DGS applied to design ultra-wide stopband low-pass filters," *IEEE Microw. Wireless Comp. Lett.*, Vol. 16, No. 5, 252–254, May 2006.

6. Geng, J.-P., J. Li, R.-H. Jin, S. Ye, X. Liang, and M. Li, "The development of curved microstrip antenna with defected ground structure," *Progress In Electromagnetics Research*, Vol. 98, 53–73, 2009.

7. Kazerooni, M., A. Cheldavi, and M. Kamarei, "Unit length parameters, transition sharpness and level of radiation in defected microstrip structure (DMS) and defected ground structure (DGS) interconnections," *Progress In Electromagnetics Research M*, Vol. 10, 93–102, 2009.

8. Naser-Moghadasi, M., G. R. Dadashzadeh, A. M. Dadgarpour, F. Jolani, and B. S. Virdee, "Compact ultra-wideband phase shifter," *Progress In Electromagnetics Research Letters*, Vol. 15, 89–98, 2010.

9. Xi, D., Y.-Z. Yin, L.-H. Wen, Y. Mo, and Y. Wang, "A compact low-pass filter with sharp cutoff and low insertion loss characteristic using novel defected ground structure," *Progress In Electromagnetics Research Letters*, Vol. 17, 133–143, 2010.

10. Fan, F. and Z. Yan, "Dual stopbands ultra-wideband antenna with defected ground structure," *Journal of Electromagnetic Waves and Applications*, Vol. 23, No. 7, 897–904, 2009.

11. Wang, C. J. and C. H. Lin, "A compact elliptic-function lowpass filter by utilizing a quasi-π-slot resonator and open stubs," *IET Microw. Antennas Propag.*, Vol. 4, No. 4, 501–511, 2010.

12. Lim, J., J. Lee, J. Lee, S. Han, D. Ahn, and Y. Jeong, "A new calculation method for the characteristic impedance of transmission lines with modified ground structures or perturbation," *Progress In Electromagnetics Research*, Vol. 106, 147–162, 2010.

13. Abdel-Rahman, A., M. S. Kheir, A. K. Verma, and A. S. Omar, "Material-loaded high Q-factor slot resonator and measurement of relative permittivity," *Progress In Electromagnetics Research C*, Vol. 13, 67–76, 2010.

14. Tirado-Mendez, J. A., H. Jardon-Aguilar, R. Flores-Leal, E. Andrade-Gonzalez, and F. Iturbide-Sanchez, "Improving frequency response of microstrip filters using defected ground and defected microstrip structures," *Progress In Electromagnetics Research C*, Vol. 13, 77–90, 2010.

15. Lin, D.-B., I.-T. Tang, and M.-Z. Hong, "A compact quad-band PIFA by tuning the defected ground structure for mobile phones," *Progress In Electromagnetics Research B*, Vol. 24, 173–189, 2010.

16. Fallahzadeh, S. and M. Tayarani, "A new microstrip UWB bandpass filter using defected microstrip structures," *Journal of Electromagnetic Waves and Applications*, Vol. 24, No. 7, 893–902, 2010.

17. Zhou, J.-M., L.-H. Zhou, H. Tang, Y.-J. Yang, J.-X. Chen, and Z.-H. Bao, "Novel compact microstrip lowpass filters with wide stopband using defected ground structure," *Journal of Electromagnetic Waves and Applications*, Vol. 25, No. 7, 1009–1019, 2011.

18. Balalem, A., A. R. Ali, J. Machac, and A. Omar, "Quasi-elliptic microstrip low-pass filters using an interdigital DGS slot," *IEEE Microw. Wireless Comp. Lett.*, Vol. 17, No. 8, 586–588, Aug. 2007.

19. Kundu, A. C. and I. Awai, "Control of attenuation pole frequency of a dual-mode microstrip ring resonator bandpass filter," *IEEE Trans. Microw. Theory Tech.*, Vol. 49, No. 6, 1113–1117, Jun. 2001.

20. Lim, J. S., C. S. Kim, D. Ahn, Y. C. Jeong, and S. Nam, "Design of low-pass filters using defected ground structure," *IEEE Trans. Microw. Theory Tech.*, Vol. 53, No. 8, 2539–2545, Aug. 2005.